ELSEVIER

Polymer 42 (2001) 3713–3722

polymer

www.elsevier.nl/locate/polymer

Chain dimensions in polysilicate-filled poly(dimethyl siloxane)

A.I. Nakatani[a,*], W. Chen[b], R.G. Schmidt[b], G.V. Gordon[b], C.C. Han[a]

[a]*Polymers Division, National Institute of Standards and Technology, 100 Bureau Dr., Stop 8542, Bldg. 224, Gaithersburg, MD 20899, USA*
[b]*Dow Corning Corporation, 2200 Salzburg Road, Midland, MI 48686, USA*

Received 12 July 2000; received in revised form 12 October 2000; accepted 12 October 2000

Abstract

We present experimental results on the single chain dimensions of isotopic blends (both mismatched and matched molecular masses) of poly(dimethyl siloxane) (PDMS) containing trimethylsilyl-treated polysilicate particles (fillers) and compare these results with Monte Carlo calculations. For polymer chains which are approximately the same size as the filler particle, a decrease in chain dimensions is observed relative to the unfilled chain dimensions at all filler concentrations. For larger chains, at low filler concentrations, an increase in chain dimensions relative to the unfilled chain dimensions is observed. Both results are in agreement with existing Monte Carlo predictions. However, at even higher filler contents, which are beyond the scope of the Monte Carlo predictions, the chain dimensions reach a maximum value before decreasing to values which are still larger than the unfilled chain dimensions. A simple excluded volume model is proposed which accounts for these observations at higher filler content.

Keywords: Small angle neutron scattering; Poly(dimethyl siloxane); Polysilicate fillers

1. Introduction

Filled polymers constitute a major portion of the commercial polymer market and have been in use since the turn of the century. In most cases, fillers are used as economical additives for altering the mechanical behavior of polymers. In spite of widespread use, a fundamental understanding of how fillers modify mechanical behavior has not been achieved. While some researchers have attempted a rigorous approach toward understanding mechanical behavior in filled polymers [1–3], empirical relationships have dominated the field. While the partial success of these empiricisms has led to some advances, knowledge of the underlying physical behavior of fillers in polymers is still lacking. One of the greatest needs in the area of filled polymers is a molecular theory of elasticity for filled polymers, analogous to kinetic theories of rubber elasticity. One potential reason for the lack of such a theory is the scarcity of data available for filled polymers on fundamental quantities such as the radius of gyration. Mark and Curro have developed a theory of rubberlike elasticity, which accounts for non-Gaussian probability distributions of chains between crosslinks [4,5]. Attempts have been made to apply this non-Gaussian theory of rubberlike elasticity to filled elastomers. Mark and coworkers [6–9] have used Monte Carlo techniques to calculate the distribution of polymer chain dimensions in the presence of filler particles. These theoretical, non-Gaussian distributions have been applied to the Mark and Curro theory to predict the stress–strain behavior and modulus of filled polymers. Experimental confirmation of these predictions are not yet available.

Small angle neutron scattering (SANS) has been used to extract dimensions of polymer chains in multicomponent mixtures. Therefore, the technique is well suited to test the predictions of Mark and coworkers on filled polymer chain dimensions. However, previous studies of polymer chain dimensions have often been restricted to deuterium labeled and unlabeled polymers in the presence of solvent or block copolymers. For filled polymer systems, studies involving a number of different scattering techniques have been reported by other investigators. Among these reports are light scattering studies of soot [10] and carbon black [11]; small angle X-ray scattering studies of filled rubbers [12–14], and organic–inorganic hybrids [15,16]; and SANS studies of silica-filled [17] and carbon black-filled [18–23] polymers. All of these studies have utilized scattering to focus on the structure and nature of the filler particles. To our knowledge, extraction of the single chain dimensions of a polymer in the presence of a filler particle has not been determined experimentally.

In this work, we present experimental results on the single

* Corresponding author. Tel.: +1-301-975-6782, fax: +1-301-975-4924.
E-mail address: alan.nakatani@nist.gov (A.I. Nakatani).

0032-3861/01/$ - see front matter
PII: S0032-3861(00)00771-0

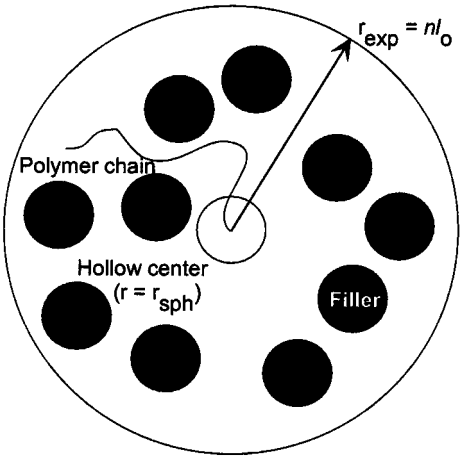

Fig. 1. Schematic representation of the Monte Carlo calculation for chain dimensions in the presence of filler particles. Based on Ref. [9], Fig. 1.

chain dimensions of isotopic blends (both mismatched and matched molecular masses) of poly(dimethyl siloxane) (PDMS) containing trimethylsilyl-treated polysilicate particles (fillers) and compare these results with the Monte Carlo calculations of Mark and coworkers. For polymer chains which are approximately the same size as the filler particle, a decrease in chain dimensions is observed relative to the unfilled chain dimensions. These results are qualitatively in agreement with the Monte Carlo calculations. For larger chains, an increase in chain dimensions at low filler concentrations relative to the unfilled chain dimensions is observed which is also in agreement with Mark and coworkers. However, at even higher filler contents, which are beyond the scope of the Monte Carlo predictions, a maximum in the chain dimensions is observed, followed by a decrease to values which are still larger than the unfilled chain dimensions. A simple excluded volume model is proposed which accounts for these observations at higher filler content.

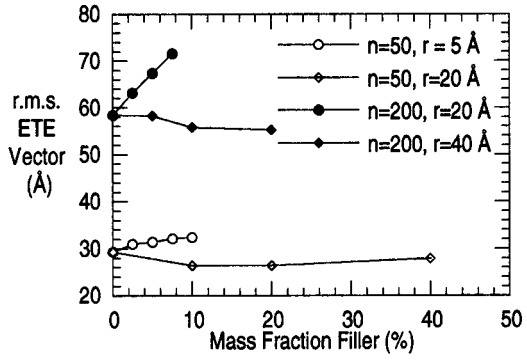

Fig. 2. Summary of the Monte Carlo calculations of PDMS chain dimensions with filler particles shown as the root-mean-squared end-to-end vector length versus mass fraction of filler (%). ○ — $n = 50$, $r_{sph} = 5$ Å; ◇ — $n = 200$, $r_{sph} = 20$ Å; ● — $n = 50$, $r_{sph} = 20$ Å; ◆ — $n = 200$, $r_{sph} = 40$ Å.

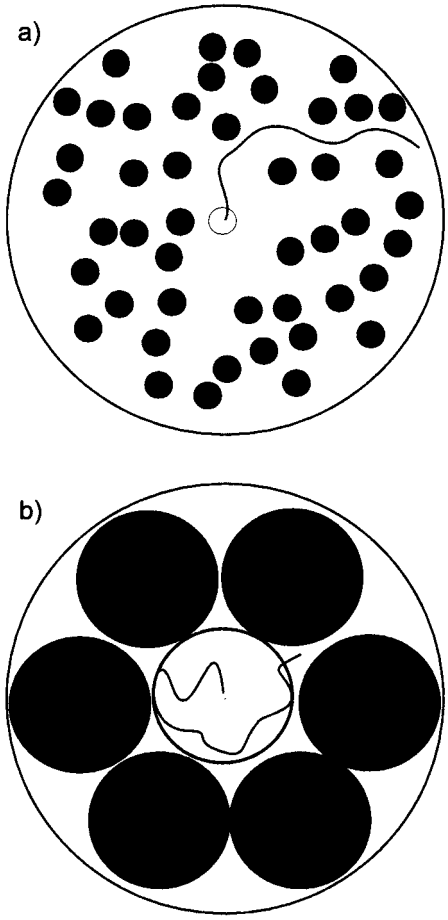

Fig. 3. Schematic of chain behavior in the presence of filler: (a) Chain much larger than the filler particle (chain expansion). (b) Chain about the same size as the filler particle (chain collapse). Drawings are schematic to show the two dimensional projections of the relative space occupied by the filler particles and polymer chain and not drawn to scale with regard to the relative sizes. Based on Ref. [9], Fig. 11.

1.1. Theoretical background

The Monte Carlo calculations by Mark and coworkers on filled, uncrosslinked polymers have suggested that the radius of gyration of the polymers is a strong function of the filler size and concentration. The Monte Carlo model adopted a rotational isomeric state model for a PDMS chain and assumed no interactions between the filler and the chain. The calculation process was initiated with a chain end located at the center of a sphere with a radius, r_{exp}, equal to the fully extended chain length ($r_{exp} = nl_0$, where n is the number of skeletal bonds and l_0 is the bond length). Filler particles were randomly placed in the interior of the sphere, with the constraint that no filler particles may occupy a volume in the center of the sphere defined by the radius of a single filler particle, r_{sph}. The filler particles were assumed to be spherical with a uniform size distribution. To obtain reasonable statistics, 30,000–500,000 conformations were generated for a given set of conditions. Any conformations generated for the polymer chain which intersected any

spherical particle were rejected in the calculation. A schematic representation of the model calculation is shown in Fig. 1.

Yuan et al. [8,9] examined PDMS chains with 50 skeletal bonds mixed with filler particles having radii of either 5 or 20 Å, and PDMS chains of 200 skeletal bonds containing filler particles with radii of either 20 or 40 Å. The results for these four cases are plotted in Fig. 2, showing the root-mean-squared end-to-end vector plotted as a function of filler concentration. For the cases where the polymer chains are much larger than the filler particles ($n = 50$, $r_{sph} = 5$ Å and $n = 200$, $r_{sph} = 20$ Å), the size of the chains increases with increasing filler concentration. However, for the cases where the polymer dimensions approach the size of the filler particles ($n = 50$, $r_{sph} = 20$ Å and $n = 200$, $r_{sph} = 40$ Å), the size of the chains decreases slightly with increasing filler concentration. These results can be understood in terms of the simple excluded volume argument shown schematically in Fig. 3. For the case where the filler particles are smaller than the polymer chain, the chain extends to the extremes of the volume defined by the sphere of radius, nl_0. Since the fillers are randomly placed in the sphere, the fillers near the center of the sphere force the chain to be more extended than if the fillers were not present (Fig. 3a). When the filler particles are nearly as large as the polymer chain (Fig. 3b), the filler particles occupy more of the space toward the periphery of the sphere, and the chain is constrained to the center. Therefore, the chain dimensions are smaller than if the fillers were not present.

1.2. Small angle neutron scattering

Akcasu et al. and Williams et al. provided a framework for extracting single chain structure factors from SANS measurements on multicomponent mixtures by the so-called high concentration method [24,25]. This method uses fixed compositions of a third component and the total amount of polymer (labeled and unlabeled) and varies the ratio of labeled to unlabeled polymer in the sample. By subtracting the appropriately weighted scattering intensities from samples with different labeling ratios, the single chain structure factor of the polymers can be obtained. This approach has been used extensively on isotopic blends of polymers with matched molecular masses in the presence of a third component.

Based on the formalism of Akcasu et al. and Williams et al., Summerfield and coworkers [26,27] and King, Ullman, and coworkers [28,29] derived the following relationship for a three component mixture of labeled and unlabeled polymers of matched molecular mass and solvent:

$$I(q,\rho) = (a_H - a_D)^2 \rho(1-\rho) S_S(q) + [a_H(1-\rho) + a_D\rho - a_s']^2 S_T(q) \quad (1)$$

where a_H, a_D, and a'_s are the monomer scattering lengths for the protonated polymer, deuterated polymer and solvent, respectively, ρ, is the fraction of total polymer which is deuterated, $S_S(q)$ is the single chain form factor, and $S_T(q)$ is the interchain form factor. Here the solvent molecule is assumed to be much smaller than the other components, hence, the structure factor for the solvent molecule, $S_{solvent}(q) = 1$. It must be emphasized that Eq. (1) is only valid for pairs of polymers with matched molecular masses. By fixing the total concentration of polymer and varying ρ one obtains a system of linear equations, which can be solved for $S_S(q)$ and $S_T(q)$. For the single chain form factors, $S_S(q)$ may be fit by a non-linear regression fitting routine to the Debye function, $g_D(x_i)$, defined by the following equation:

$$g_D(x_i) = (2/x_i^2)[\exp(-x_i^2) - 1 + x_i^2] \quad (2)$$

where $x_i = q^2 N_i b^2/6$, N_i is the degree of polymerization of the polymer, and b is the statistical segment length, yielding R_g of the polymer chains ($R_g = N_i b^2/6$). Alternatively, by plotting $1/S_S(q)$ against q^2, a straight line results and R_g may be calculated from the slope and intercept of the line based on the following relation:

$$1/S_S(q) = \text{const.}(1 + q^2 R_g^2/3) \quad (3)$$

Because of the assumption of matched molecular masses of the polymers, one single chain form factor is obtained which is assumed to apply to both the labeled and unlabeled polymer.

Tangari, Summerfield and coworkers [30–32] examined the effects of mismatched molecular masses on the high concentration method. However, the presence of a third component was not considered in their treatment. The result is analogous to the results obtained for isotopic blends with matched molecular masses except the single chain form factor is the weighted sum of the individual form factors for the deuterated and protonated polymer chains:

$$S_S(q) = [\rho S_S^H(q) + (1-\rho) S_S^D(q)] \quad (4)$$

where $S_S^H(q)$ is the single chain form factor for the protonated polymer and $S_S^D(q)$ is the single chain form factor for the deuterated polymer. The primary assumption in the approach of Tangari and coworkers is that the system is non-interacting. This assumption helps to eliminate a number of crossterms in the final expression for the total scattering intensity.

In this work, we obtained experimental results on the single chain dimensions of isotopic blends of PDMS with polysilicate fillers by using a treatment similar to Tangari and coworkers. Our principal assumption was that the polysilicate filler may be effectively treated as a solvent molecule. The polysilicate used in this work is smaller than traditional reinforcing fillers and is a liquid which flows at room temperature, but exhibits brittle, glass-like behavior below −70°C. Therefore, the polysilicate is not like most traditional fillers that are rigid, macroscopic particles which come in powder form. However, the polysilicate

Table 1
Homopolymer characteristics (M_0, M_w and M_n are the monomer, mass average, and number average molecular masses, respectively, in g/mol. DP_w is the mass average degree of polymerization obtained from M_w, and R_g is the radius of gyration obtained from dilute solution SANS measurements)

Polymer	M_0	M_w (SEC)	M_w/M_n(SEC)	DP_w	M_w (Zimm)	R_g (Å)	A_2(mol cm^3/g^2)
100DP h-PDMS	74	12.0×10^3	1.05	160	15.8×10^3	33.6	6.92×10^{-4}
					$\pm 1.0\times10^3$	$\pm$ 1.0	$\pm 0.50\times10^{-4}$
100DP d-PDMS	80	38.1×10^3	2.50	476	34.7×10^3	76.5	5.20×10^{-4}
					$\pm 6.0\times10^3$	$\pm$ 5.0	$\pm 0.70\times10^{-4}$
1000DP h-PDMS	74	85.7×10^3	3.82	1160	89.9×10^3	110.0	5.50×10^{-4}
					$\pm 15.0\times10^3$	$\pm$ 5.0	$\pm 0.40\times10^{-4}$
1000DP d-PDMS	80	81.7×10^3	4.16	1021	85.4×10^3	114.1	3.10×10^{-4}
					$\pm 8.0\times10^3$	$\pm$ 7.0	$\pm 0.60\times10^{-4}$
Polysilicate filler	72	1.9×10^{3a}	1.23	26	5.7×10^3	10.6	3.47×10^{-3}
					$\pm 1.0\times10^3$	$\pm$ 1.5	$\pm 0.38\times10^{-3}$

[a] A_2 values are for the polymer in toluene (toluene-d_8 for protonated samples, toluene h_8 for deuterated samples). $\pm$ values for Zimm M_w, R_g and A_2 are derived from standard error estimates of the slope and intercept values from linear regression fits to the extrapolated $c = 0$ and $q = 0$ lines of the Zimm plots.

significantly alters the mechanical behavior of PDMS polymers. The assumption that the polysilicate can be treated as a solvent molecule allows the analysis scheme of Tangari and coworkers to be combined with the results of Summerfield, King, Ullman and coworkers to give the following expression for the scattering intensity:

$$I(q,\rho) = (a_H - a_D)^2\rho(1-\rho)[\rho S_S^H(q) + (1-\rho)S_S^D(q)] + [a_H(1-\rho) + a_D\rho - a_s']^2 S_T(q) \quad (5)$$

Eq. (5) will be utilized as the basis for extracting the polymer single chain form factors in this study. The function, $S_T(q)$, which is extracted through this analysis is the form factor which contains the third component. We assume our filler can be treated as a solvent molecule to apply the data reduction scheme of Summerfield et al. This is true as long as the filler particle dimension is sufficiently small to justify the assumption that $S_{solvent}(q) = 1$. However, it should be noted that the form factor for the third component is contained in $S_T(q)$ regardless of the assumption we make for the physical state of the third component.

For comparison, the radius of gyration values for the polymers were measured in dilute toluene solutions (near theta conditions) and in the bulk isotopic blend without filler. The radii in the bulk isotopic blends were also examined as a function of the ratio of labeled to unlabeled polymer. The results for the isotopic blends were analyzed using the standard two-component random phase approximation (RPA) theory [33]:

$$S(q) = k_N\{[\phi_A v_A N_A g_D(x_A)]^{-1} + [\phi_B v_B N_B g_D(x_B)]^{-1} + (2\chi/v_0)\}^{-1} + \text{Baseline} \quad (6)$$

where N_i is the degree of polymerization index, ϕ_i the volume fraction, v_i the molar volume of the ith component, v_0 a reference volume and, k_N is the contrast factor given as:

$$k_N = N_0[(a_A/v_A) - (a_B/v_B)]^2 \quad (7)$$

In Eq. (7), N_0, a_i, and v_i are, respectively, Avogadro's number, the scattering length and molar volume of a monomer unit of the ith component. For polydisperse materials, in Eq. (6), the N_i are replaced by $\langle N_i\rangle_n$, the number average degree of polymerization and the Debye functions, $g_D(x_i)$ are replaced by the mass average Debye function given by Eq. (8), assuming a Schultz–Zimm distribution for the molecular masses:

$$\langle g_D(x_i)\rangle_w = (2/x_i^2)\{x_i - 1 + [h/(h + x_i)]h\} \quad (8)$$

where, $x_i = q^2\langle N_i\rangle_n b^2/6$, $h = [\langle N_i\rangle_w/\langle Ni\rangle_n - 1]^{-1}$ and $\langle N_i\rangle_w$ is the mass average degree of polymerization. The nonlinear regression fitting routine to the RPA equation accounting for the molecular mass distributions of both polymers was performed with b, χ/v_0 and the incoherent baseline as floating parameters. A single value of b is obtained which is an average value for both of the polymers. Based on the values for the degree of polymerization obtained independently by SEC for each polymer, the R_g of each polymer is obtained according to the relation, $R_g = (\langle N_i\rangle_w b^2/6)^{1/2}$. The radius of gyration values are calculated based on the mass average degree of polymerization.

2. Experimental

2.1. Materials

The PDMS polymers (density = 0.97 g/cm^3) used in this study were provided by Dow Corning Corporation.[1] Deuterated PDMS (d-PDMS) was synthesized via the hydrolysis and condensation of perdeuterated chlorosilanes. The molecular masses were characterized independently by size-exclusion chromatography (SEC) using PDMS standards.

[1] Certain equipment and instruments or materials are identified in this paper in order to adequately specify the experimental details. Such identification does not imply recommendation by the National Institute of Standards and Technology nor does it imply the materials are the best available for the purpose.

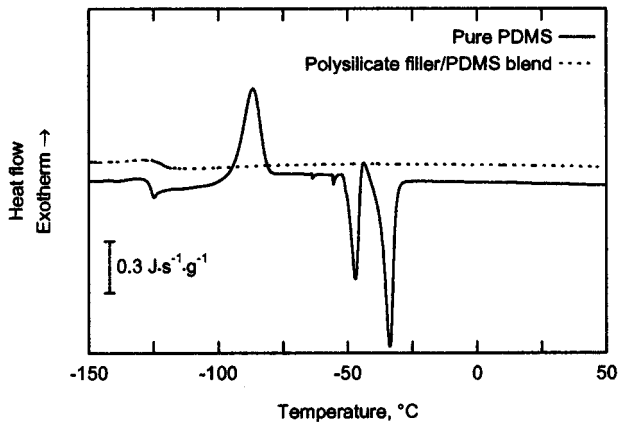

Fig. 4. DSC thermogram for a polysilicate filler/PDMS blend containing a mass fraction of 50% filler. The crystallization of PDMS is inhibited and a single T_g which is slightly higher than the T_g of the pure PDMS is observed.

Typical uncertainties on the values of M_w obtained by SEC are ±5%. Four different polymers were available for this study and were designated as 100DP h-PDMS, 100DP d-PDMS, 1000DP h-PDMS, and 1000DP d-PDMS corresponding to low molecular mass protonated and deuterated PDMS and high molecular mass protonated and deuterated PDMS, respectively. Table 1 gives the characteristics of the polymers. It is important to note that there is actually a large mismatch in molecular mass between the 100DP h-PDMS and the 100DP d-PDMS. This mismatch necessitated the application of the data analysis scheme for mismatched molecular mass polymers in solvent described above.

The trimethylsilyl-treated polysilicate material ($M_n = 1500$ g/mol by SEC, density = 1.05 g/cm^3) was synthesized via the co-hydrolysis and condensation of hexamethylsiloxane and a tetraalkoxysilane at a mole ratio of 1.2:1. The resulting material has a composition of $(Me_3SiO_{1/2})_{0.54}(HOSiO_{3/2})_{0.02}(EtOSiO_{3/2})_{0.03}(SiO_{4/2})_{0.41}$ (Subscripts indicate mass fractions of each structural unit). The trimethylsilyl treatment of the polysilicate renders the particle surface non-reactive, thereby enhancing the particle size stability. By reacting with surface silanol groups and lowering the surface energy of the filler, the trimethylsilyl treatment also improves the compatibility of the filler with the PDMS. The polysilicate material has a non-linear, amorphous, particulate structure. At low temperatures these materials exhibit glassy behavior but display a rapid decrease in modulus near their effective glass transition temperature (T_g) of −70°C (as determined by dynamic mechanical thermal analysis). Since the molar mass of the polysilicate filler is relatively low and the structure is compact, the filler does not exhibit any signs of molecular entanglement during the transition from a glassy to a liquid material near T_g. Fig. 4 compares differential scanning calorimetry (DSC) heating traces of the 100DP h-PDMS polymer with a blend of the polysilicate and 100DP h-PDMS containing a mass fraction of 50% polysilicate. Experiments were conducted on a TA Instruments 2920 DSC[1] at a scan rate of 10°C/min. Introduction of the polysilicate to the linear polymer component results in an increase in T_g of roughly 4°C (T_g (PDMS) = −127°C and T_g (Blend) = −124.5°C) and a dramatic reduction in the crystallization of the h-PDMS component. Owing to their particulate shape and the large impact of PDMS crystalline domain retardation on the properties of PDMS-based networks below −50°C, the polysilicate materials in this study are referred to as non-reinforcing fillers. The effect of the filler is to modify the release properties by increasing the force (energy) required to peel a release liner from a pressure-sensitive adhesive [34].

Since the polymers have low glass transition temperatures and low viscosities, mixtures of the protonated and deuterated polymers and the polysilicate filler were prepared by weighing the appropriate amounts of each component in a screw-top vial and placing the vials on a roller at ambient temperature to mechanically mix the samples. The rolling speed was approximately one revolution per minute and the samples were mixed for 24 h. Five different filler concentrations for the 100DP blends and the 1000DP blends were prepared. At each filler concentration, 5 or 6 different ratios of protonated to deuterated polymer were prepared so that multiple solutions to the systems of linear equations were available.

2.2. Small angle neutron scattering

SANS measurements were carried out at the Cold Neutron Research Facility of the NIST Center for Neutron Research. Data were collected on the 8 m SANS instrument with the neutron wavelength, $\lambda = 12.0$ Å, and a sample-to-detector distance of 3.6 m, giving a q range of 0.008–0.065 Å^{-1}. The samples for solution characterization SANS measurements were contained in 2 mm pathlength quartz cells for liquids, while the remaining samples were placed in either 1 mm pathlength quartz cells (100DP blends) or sandwiched between quartz windows with a 0.5 mm spacer (1000DP blends). Data were collected over a two-dimensional detector and corrected for dark current intensity due to electronic and background neutron noise and empty cell scattering. Background scattering, mainly due to incoherent scattering, of the protonated components (both the protonated PDMS and the polysilicate filler) in the samples were subtracted separately during the data reduction. Absolute intensity calibration was done with a dry silica gel as a secondary standard, calibrated in terms of a primary vanadium standard.

3. Results

3.1. SANS solution characterization

The solution characterization of all components was conducted by a standard Zimm-type analysis [35] where the scattering from low concentration solutions of each

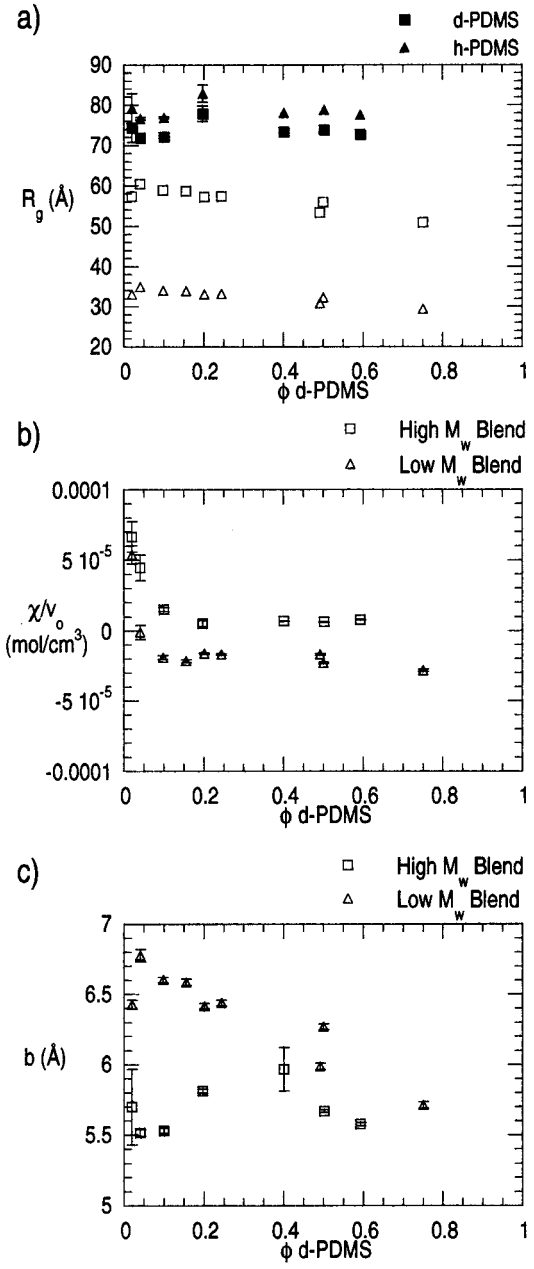

Fig. 5. (a) Variation of R_g as a function of d-PDMS concentration for the isotopic, unfilled blends. Open symbols represent data for the 100DP blend, closed symbols represent data for the 1000DP blend. (b) Variation of χ/v_0 as a function of d-PDMS concentration for the isotopic, unfilled blends. (c) Variation of the average statistical segment length, b, as a function of d-PDMS concentration for the isotopic, unfilled blends.

component (volume fractions of 0.01, 0.02, 0.03 and 0.05) in toluene were measured. For the unlabeled species, perdeuterated toluene was used as the solvent, and for the labeled species, protonated toluene was used as the solvent. Plots of the concentration-weighted inverse scattering intensity, $ck_N/I(q)$, versus q^2 were constructed, where $q = (4\pi/\lambda)\sin(\theta/2)$, θ is the scattering angle and k_N is the scattering contrast factor given by Eq. (7).

From the zero concentration and zero scattering angle extrapolations of the $ck_N/I(q)$ versus q^2 plots, the mass average molecular mass, M_w,[2] the radius of gyration, R_g, and second virial coefficient, A_2, were obtained. These results are compared to the SEC data given in Table 1. The agreement between the SEC and SANS values for M_w is reasonably good in most cases. The largest discrepancy in M_w occurred for the polysilicate filler. The polysilicate filler was also characterized by matrix-assisted laser desorption/ionization time-of-flight (MALDI-TOF) mass spectrometry and a value for M_w of 6.5×10^3 g/mol was obtained, which is consistent with the SANS results ($M_w = 5.7 \times 10^3$ g/mol). Since the polysilicate filler is believed to be a highly branched material and the molecular mass determination by SEC is dependent on polysilicate filler standards related to linear PDMS standards, the calibration of the SEC may be responsible for the discrepancies in M_w of the filler. The R_g value for the filler of 10.6 Å is much smaller than the solution R_g values of any of the polymer components, therefore, our primary assumption that the filler particle can be treated as a solvent molecule is satisfied.

The second virial coefficient values of the protonated polymer/deuterated solvent pairs are slightly greater than the values for the deuterated polymer/protonated solvent pairs and are consistent with values reported previously in the literature [36]. The slight differences are an indication that the two polymers will not be completely non-interacting due to the isotopic labeling. The A_2 values also demonstrate a slight decrease with increasing molecular mass. This trend is also consistent with the molecular mass dependence of A_2 for PDMS in toluene observed previously. The positive values for A_2 indicate the polymers are slightly swollen in the solvents compared to their Θ dimensions. The A_2 value for the polysilicate filler in toluene is larger than the polymer A_2 values, indicating a difference in the filler–solvent interaction strength compared to the polymer–solvent interaction. This also implies that the three component mixture of protonated and deuterated polymers and filler is not completely non-interacting (Θ conditions). Since the existence of Θ conditions is assumed for the data analysis scheme described in the introduction, complications are possible in the three component data reduction.

3.2. Unfilled bulk polymer chain dimensions

The scattering from the 100DP and 1000DP isotopic blends was measured and the scattering profiles, $S(q)$, were analyzed by fitting the experimental data to the RPA (Eq. (6)) using a non-linear least squares regression routine. The polydispersity values listed in Table 1 were incorporated into the fits

[2] According to ISO 31-8, the term Molecular Mass has been replaced by Relative Molecular Mass, symbol M_r. Thus, if this nomenclature and notation were to be followed, one would write, $M_{r,n}$, instead of the historically conventional M_n for the number average molecular weight and it would be called the Number Average Relative Molecular Mass. The conventional notation, rather than the ISO notation, has been employed for this publication.

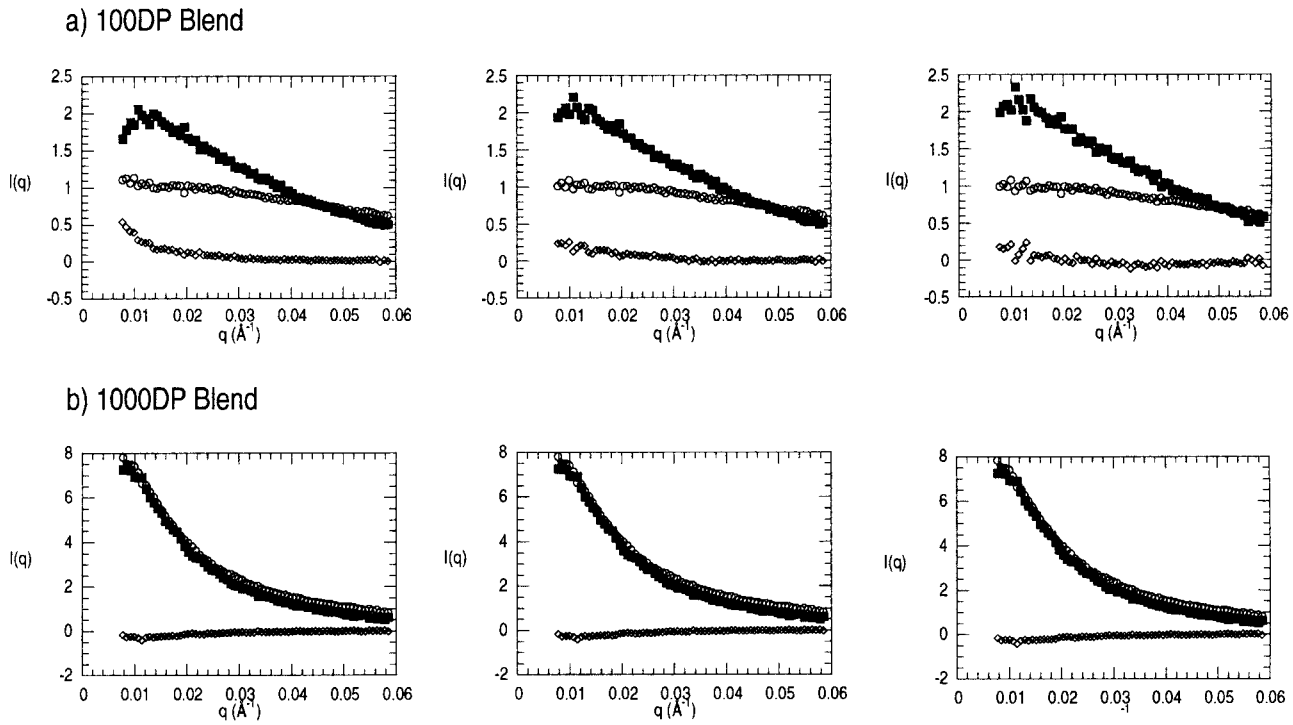

Fig. 6. Examples of $S_S^H(q)$, $S_S^D(q)$, and $S_T(q)$ obtained for the: (a) 100DP blend with 10% mass fraction filler. (b) 1000DP blend with 20% mass fraction filler. ○ — $S_S^H(q)$; ■ — $S_S^D(q)$; ◇ — $S_T(q)$.

according to Eq. (8). From the values obtained for the average segment length, b, and the degrees of polymerization for each polymer obtained by SEC, the R_g values of both the deuterated and protonated polymer in the isotopic mixtures were obtained. A number of different ratios of deuterated to protonated polymer were prepared so that the composition dependence of R_g could be examined for each isotopic blend as shown in Fig. 5. In this figure and all subsequent figures, the vertical bars on the data points represent ±one standard deviation, unless noted otherwise. The results for the 100DP blend are smoother than the results for the 1000DP blends. This may be due to a higher degree of uncertainty in the degree of polymerization and the large polydispersity indices of the 1000DP polymers. The variations of χ/v_0 and b as a function of the d-PDMS concentration are also shown in Fig. 5. The values of R_g in the bulk, unfilled blends are lower than the values obtained from the Zimm plots for the solutions of the homopolymers. This is anticipated since the PDMS chains swell in the presence of toluene. The χ/v_0 values are very close to zero, while the calculated values for χ/v_0 at the spinodal temperature, χ_{sp}/v_0, are on the order of 0.01 mol/cm^3, which is nearly four orders of magnitude larger than the fit values obtained for χ/v_0. This indicates these blends are far from phase separating and the experiments were conducted well into the miscible region of the phase diagram. We also noted no systematic variation of the fit parameters as a function of temperature between 30 and 90°C, which we also interpret as an indication that the two polymers are completely miscible with no strong interactions.

Some concentration dependence of R_g and the associated parameters, χ/v_0 and b were observed in the isotopic blends, which was not anticipated. One would expect no such concentration dependence for blends of two polymers which only vary in their hydrogen or deuterium contents. However, variations b and χ/v_0 as a function of the degree of polymerization have been observed in other isotopic blends of PDMS by Beaucage et al. [37] and the concentration dependence of χ/v_0 been discussed for other polymers recently by Crist [38]. While the discussion of this behavior is beyond the scope of this paper, the presence of this concentration dependence in R_g complicates the determination of the unfilled chain dimensions. Only a range of unfilled R_g values can be compared to the filled R_g values, since the experiments on the three component mixtures were performed at fixed ratios of total polymer to filler with varying ratios of labeled to unlabeled polymer. Significant changes in the chain dimensions in the presence of filler will be more difficult to determine because of this concentration dependence in R_g.

3.3. Filled polymer chain dimensions

Various compositions of three component mixtures were used in this study. For the filled 100DP mixtures, five different ratios of labeled to unlabeled chains were examined. For the solution to three linear equations and three unknowns, these five different labeling ratios provide 10 different solutions for each of the three unknowns (S_S^H, S_S^D, and S_T). Due

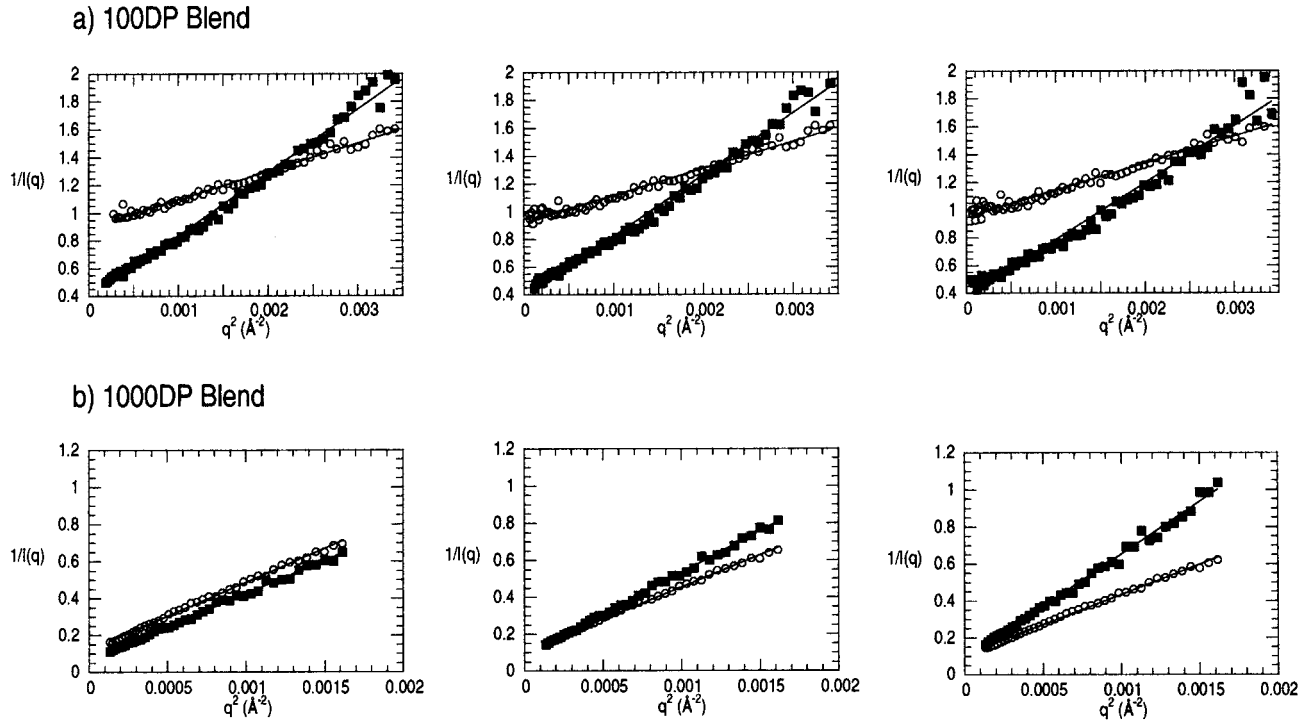

Fig. 7. Examples of the linear fits to $1/S_S^i(q)$ versus q^2 for the: (a) 100DP blend with 10% mass fraction filler. (b) 1000DP blend with 20% mass fraction filler. ○ — $1/S_S^H(q)$; ■ — $1/S_S^D(q)$.

to the polydispersity of the 1000DP samples, six different labeling ratios were measured for most concentrations of the filler. This allowed us to obtain 20 different solutions to the system of linear equations. Examples for 3 of the 10 solutions to S_S^H, S_S^D, and S_T for the 100DP samples with a filler mass fraction of 10% are shown in Fig. 6a. All concentrations of filler are expressed as mass fraction unless noted otherwise. Examples for 3 of the 20 solutions to S_S^H, S_S^D, and S_T for the 1000DP samples with 20% filler are shown in Fig. 6b. As expected for polymers of different molecular mass, the single chain form factors for the 100DP polymers are distinct, while the single chain form factors for the 1000DP polymers of matched molecular mass are similar. For all filler concentrations, the results presented below are

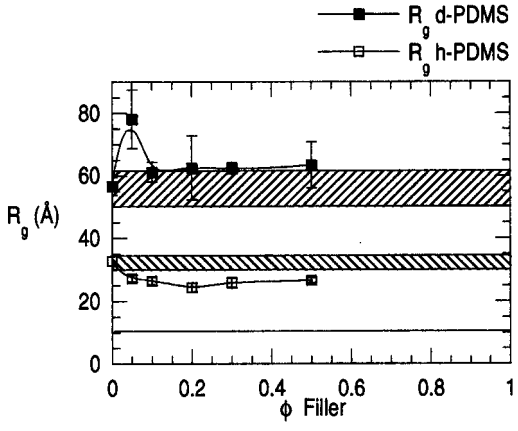

Fig. 8. Apparent R_g values of 100DP d-PDMS and 100DP h-PDMS as a function of polysilicate filler concentration. Bars in figures represent ± one standard deviation in the measurements assuming normal, random statistical errors. Solid line indicates the R_g value for the polysilicate. Crosshatched areas indicate the range of R_g values for each component in the unfilled blend obtained from the RPA analysis. //// — h-PDMS R_g range; \\\\ — d-PDMS R_g range.

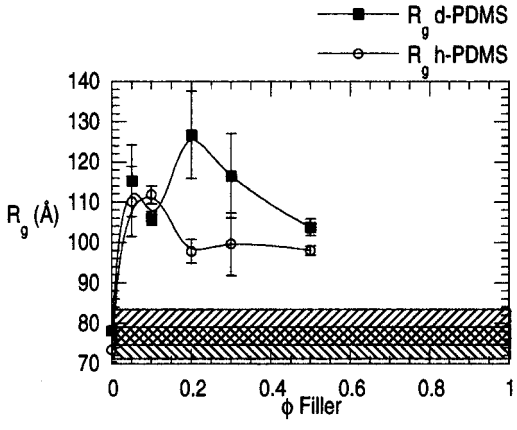

Fig. 9. Apparent R_g values of 1000DP d-PDMS and 1000DP h-PDMS as a function of polysilicate filler concentration. Bars in figures represent ± one standard deviation in the measurements assuming normal, random statistical errors. Crosshatched areas indicate the range of R_g values for each component in the unfilled blend obtained from the RPA analysis. //// — h-PDMS R_g range; \\\\ — d-PDMS R_g range.

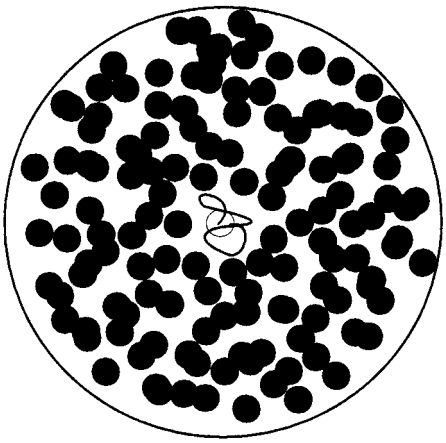

Fig. 10. Proposed model for chain behavior in the presence of filler for chains much larger than the filler particle at high filler concentrations (chain collapse). Drawing is schematic to show the two dimensional projections of the relative space occupied by the filler particles and polymer chain and not drawn to scale with regard to the critical volume fraction or relative size scales.

the mean values obtained from the solutions to the systems of linear equations.

The solutions to the systems of linear equations were used to construct plots of $1/S_S^i$ against q^2. Linear fits to Eq. (2) were done to obtain the R_g values. The fit range for the 100DP samples was $0.015\ \text{Å}^{-1} < q < 0.060\ \text{Å}^{-1}$ and the range for the 1000DP samples was $0.010\ \text{Å}^{-1} < q < 0.040\ \text{Å}^{-1}$. Examples of the linear fits corresponding to the data shown in Fig. 6 are shown in Fig. 7. As stated previously, for the mismatched molecular mass pair, lines with different slope and intercept values were anticipated for the labeled and unlabeled polymer, while lines with approximately the same slope and intercept were expected for the matched molecular mass polymers. At each filler concentration, the mean of the R_g values obtained from all the linear fits was used to determine the chain dimensions as a function of filler concentration discussed below.

The variation in R_g as a function of filler concentration is shown in Figs. 8 and 9 for the 100DP blend and 1000DP blend, respectively. The vertical bars on the data points represent ±one standard deviation and the solid lines represent smooth curve fits to the data as a guide to the eye. In each plot, the range of R_g values for the unfilled polymers obtained from the RPA fits described above are shown by the crosshatched areas. For the 100DP results, the R_g value of the filler is also shown by the solid line. In the low molecular mass mixture, the 100DP h-PDMS shows a slight decrease in R_g with increasing filler concentration. This decrease appears to be significant since all values and the associated errors lie below the range of unfilled R_g values. The 100DP d-PDMS shows much different behavior. The value of R_g first increases drastically at low filler content (mass fraction of 5%), then decreases to values which appear to be slightly larger than the unfilled R_g. However, the standard errors on the values for the 100DP d-PDMS are much larger than for the 100DP h-PDMS, therefore, beyond the initial increase in chain dimensions at 5% filler, the chain dimensions at higher filler contents are statistically the same as the unfilled chain dimensions.

In Fig. 9, both the 1000DP h-PDMS and the 1000DP d-PDMS R_g values behave similarly as a function of filler concentration. The behavior is also similar to the behavior of the 100DP d-PDMS described above. At low filler contents, the R_g values of both the h- and d-PDMS increase and then at higher concentrations the R_g values decrease. However, the dimensions at higher filler contents remain significantly greater than the unfilled chain dimensions. While the general behavior of both polymers is similar, there appears to be a slight difference between the protonated and deuterated polymer. For the 1000DP h-PDMS, the maximum R_g value appears to occur around a filler content of 10%, whereas the maximum R_g value for the 1000DP d-PDMS appears to occur at a filler concentration of 20%. The R_g values for the 1000DP h-PDMS for filler mass fractions equal to 20% or larger are all approximately the same, while the R_g values for the d-PDMS decrease gradually between filler concentrations of 20–50%.

The q ranges utilized in Fig. 7 to extract the R_g values shown in Figs. 8 and 9 do not completely satisfy the condition $qR_g < 1$. Ullman [39] has analyzed the errors when this condition is not satisfied and estimates errors as large as 20% are possible. These types of errors may be associated with the R_g values extracted from Fig. 7, however, by fitting the data over a consistent q range, we are confident in the relative variation in R_g values with respect to filler concentration.

4. Discussion

The SANS determination of R_g as a function of filler content measured in this study has some qualitative resemblance to the Monte Carlo calculations of chain dimensions in the presence of spherical particles by Mark and coworkers. Although the two main assumptions that the filler particle used in our samples can be treated as a solvent molecule and that all components are non-interacting may not be rigorously correct, the polymer R_g values obtained in the filled samples appear to be reasonable. For the polymer with chain dimensions that approach the dimensions of the filler (100DP h-PDMS), the decrease in chain dimensions with increasing filler content is similar in magnitude to the change predicted by the Monte Carlo calculations.

For the cases where the polymer chain dimension is larger than the dimension of the filler particle, Yuan et al. [8,9] only performed calculations up to filler concentrations of 10% compared to our results on samples containing up to 50% filler (Fig. 2). Higher concentrations of filler were not considered by Yuan et al. due to the small number of chain conformations which could be generated successfully. While the Monte Carlo calculations for polymer chains

much larger than the filler particles, show a monotonic increase of the chain dimensions in the filled samples with increasing filler content (Fig. 2), our results (Figs. 8 and 9) seem to indicate that the chain dimensions reach a maximum at low filler contents then decrease at higher filler concentrations. However, at all filler contents, the chain dimensions are greater than the unfilled chain dimensions.

Since our samples contain filler concentrations much higher than mass fractions of 10%, it is possible that the trend in our SANS data would be observed in calculations performed at higher filler contents. An extension of the schematic shown in Fig. 3a may provide an explanation for our results. In Fig. 3a, the filler concentration is sufficiently low, so that chain expansion is observed. However, if the concentration of small filler particles increases to the point where they begin to touch and interconnect (Fig. 10), the picture becomes similar to the case shown in Fig. 3b. Because of the excluded volume of the particles, a large portion of the volume defined at the start of the calculation is unavailable to the chain, and the chain goes from an expanded state (Fig. 3a) to a collapsed state (Fig. 10). Extension of the Monte Carlo calculations to test this hypothesis would be desirable, however, with the constraints on the computational time involved, such an extension does not seem likely.

5. Conclusions

We have measured polymer chain dimensions in the presence of filler particles as a function of filler concentration by SANS. The behavior of these chain dimensions as a function of filler concentration and filler size are in qualitative agreement with the predictions made by Monte Carlo calculations. Similar measurements on larger polysilicate fillers as a function of the particle size and concentration may be feasible and extension of these studies to more traditional filler materials such as fumed silica or fibers may also be possible. These results have implications in relation to filled polymer networks, as well. If measurements of this type could be performed on undeformed and deformed, crosslinked systems, the necessary molecular level information necessary for a molecular theory of elasticity for filled networks may be possible.

Acknowledgements

We wish to gratefully acknowledge many useful discussions with Drs B.J. Bauer and B. Hammouda of NIST and Dr A.Z. Ackasu of the University of Michigan concerning the data treatment for the three component mixtures. In addition, the preparation and purification of deuterated siloxane monomers, and polymerization were completed by A.P. Wright, B. Zhong, T.M. Leaym, G.M. Wieber and R.G. Taylor of Dow Corning and greatly appreciated. The work of Drs W.E. Wallace and C.M. Guttman of NIST to measure the MALDI-TOF mass spectrum of the polysilicate sample is also greatly appreciated.

References

[1] Kluppel M, Heinrich G. Rubber Chem Tech 1995;68:623.
[2] Heinrich G, Vilgis TA. Macromolecules 1993;26:1109.
[3] Witten TA, Rubinstein M, Colby RH. J Phys II France 1993;3:367.
[4] Mark JE, Curro JG. J Chem Phys 1983;79:5705.
[5] Curro JG, Mark JE. J Chem Phys 1984;80:4521.
[6] Kloczkowski A, Sharaf MA, Mark JE. Chem Engng Sci 1994;49:2889.
[7] Sharaf MA, Kloczkowski A, Mark JE. ACS Polym Preprints 1995;36:368.
[8] Yuan QW, Kloczkowski A, Sharaf MA, Mark JE. ACS PMSE Preprints 1995;73:374.
[9] Yuan QW, Kloczkowski A, Mark JE, Sharaf MA. J Polym Sci, Polym Phys Ed 1996;34:1647.
[10] Mountain RD, Mulholland GW. Langmuir 1988;4:1321.
[11] Bezot P, Hesse-Bezot C, Rousset B, Diraison C. Colloids Surf, A 1995;97:53.
[12] Schmidt PW. J Appl Crystallogr 1982;15:567.
[13] Young RJ, Al-Khudhairy DHA, Thomas AG. J Mater Sci 1986;21:1211.
[14] Karásek L, Sumita M. J Mater Sci 1996;31:281.
[15] Landry MR, Coltrain BK, Landry CJT, O'Reilly JM. J Polym Sci, Part B: Polym Phys 1995;33:637.
[16] Jackson CL, Bauer BJ, Nakatani AI, Barnes JD. Chem Mater 1996;8:727.
[17] Freltoft T, Kjems JK, Sinha SK. Phys Rev B 1986;33:269.
[18] Wignall GD, Farrar NR, Morris S. J Mater Sci 1990;25:69.
[19] Salomé L, Carmona F. Carbon 1991;29:599.
[20] Hjelm RP, Seeger PA, Wampler WA. Polym Polym Compos 1993;1:53.
[21] Salomé L. J Phys II France 1993;3:1647.
[22] Hjelm RP, Wampler WA, Seeger PA, Gerspacher M. J Mater Res 1994;9:3210.
[23] Marr DWM, Wartenberg M, Schwartz KB, Agamalian MM, Wignall GD. Macromolecules 1997;30:2120.
[24] Akcasu AZ, Summerfield GC, Jahshan SN, Han CC, Kim CY, Yu H. J Polym Sci, Polym Phys Ed 1980;18:863.
[25] Williams CE, Nierlich M, Cotton JP, Jannink G, Boué F, Daoud M, Farnoux B, Picot C, deGennes PG, Rinaudo M, Moan M, Wolff C. J Polym Sci, Polym Lett Ed 1979;17:379.
[26] Jahshan SN, Summerfield GC. J Polym Sci, Polym Phys Ed 1980;18:1859.
[27] Jahshan SN, Summerfield GC. J Polym Sci, Polym Phys Ed 1980;18:2415.
[28] King JS, Boyer W, Wignall GD, Ullman R. Macromolecules 1985;18:709.
[29] Ullman R, Benoit H, King JS. Macromolecules 1986;19:183.
[30] Tangari C, Summerfield GC, King JS, Berliner R, Mildner DFR. Macromolecules 1980;13:1546.
[31] Summerfield GC. J Polym Sci, Polym Phys Ed 1981;19:1011.
[32] Tangari C, King JS, Summerfield GC. Macromolecules 1982;15:132.
[33] de Gennes PG. Scaling concepts in polymer physics. Ithaca: Cornell University Press, 1979.
[34] Gordon GV, Schmidt RG. J Adhes 2000;72:133.
[35] Tanford C. Physical chemistry of macromolecules. New York: Wiley, 1961.
[36] Brandrup J, Immergut EH. Polymer handbook. 3rd ed. New York: Wiley, 1989 (p. VII-134).
[37] Beaucage G, Sukumaran S, Clarson SJ, Kent MS, Schaefer DW. Macromolecules 1996;29:8349.
[38] Crist B. J Polym Sci, Part B: Polym Phys 1997;35:2889.
[39] Ullman R. J Polym Sci, Part B: Polym Phys Ed 1985;23:1477.